

# PHOTOACOUSTIC PHASE ANGLE FOR NONINVASIVE MONITORING OF MICROCIRCULATORY CHANGE IN HUMAN SKIN: A PRELIMINARY INVESTIGATION

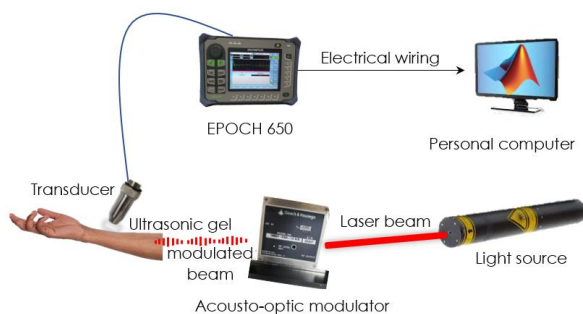
Hui Ling Chua, Audrey Huong\*

Department of Electronic Engineering, Faculty of Electrical and Electronic Engineering, Universiti Tun Hussein Onn Malaysia, Parit Raja, Batu Pahat, Johor, Malaysia

**Article history**  
Received  
22 November 2021  
Received in revised form  
27 March 2022  
Accepted  
7 April 2022  
Published Online  
20 June 2022

\*Corresponding author  
audrey@uthm.edu.my

## Graphical abstract



## Abstract

Tissue oxygen monitoring systems, such as pulse oximeter, is unreliable in patients with compromised microcirculation. Modern imaging modalities such as Magnetic Resonance Imaging (MRI) offer good diagnostic accuracy at the expense of increased cost and complexity in their operations. This paper studies the use of photoacoustic (PA) phase change as a predictor of skin tissue oxygen levels. We used EPOCH 650 ultrasonic flow detector with a longitudinal transducer for measurement of PA waves. This pilot study was conducted on six human subjects. The produced ultrasonic waves were collected from their anterior left arm under three experimental conditions, namely at rest, venous and arterial blood flow occlusions, for determination of hemoglobin absorption dependent phase change in tissue. The overall mean and standard deviation (STDEV) of phase angles for at rest condition are calculated as  $1.43 \pm 0.06$  radians (rads). Higher phase angles are determined for diastolic and systolic occlusion pressures given by  $1.69 \pm 0.05$  rads and  $2.09 \pm 0.06$  rads, respectively. This work concluded that the feasibility of our PA system to monitor changes in tissue oxygen performance renders it a promising alternative for portable assessment and measurement of oxygen concentration within microcirculation environment.

**Keywords:** Photoacoustic, phase angle, tissue oxygen, microcirculatory, portable

## Abstrak

Sistem pemantauan oksigen tisu, seperti pulse oximeter, tidak boleh dipakai pada pesakit yang mempunyai peredaran mikro. Sistem yang lain seperti pengimejan resonans magnet menawarkan ketepatan diagnostik yang tinggi, dengan kos yang tinggi dan kerumitan dalam operasinya. Kajian ini dengan matlamat untuk mengatasi masalah dengan mencadangkan penggunaan perubahan fasa fotoakustik (PA) sebagai peramal tahap oksigen tisu kulit. Kerja ini menggunakan pengesan ultrasonik EPOCH 650 dengan transduser untuk pengukuran isyarat PA. Kajian ini melibatkan enam orang subjek manusia. Gelombang tekanan dikumpulkan dari lengan kiri anterior mereka dalam tiga keadaan eksperimen, iaitu pada waktu rehat, oklusi aliran darah vena dan arteri, untuk pengekstrakan maklumat fasa bergantung

penyerapan hemoglobin. Purata dan sisihan piawai keseluruhan (STDEV) sudut fasa untuk keadaan rehat dikira sebagai  $1.43 \pm 0.06$  radian (rad). Sudut fasa yang lebih tinggi dibuktikan pada tekanan oklusi diastolik dan sistolik yang masing-masing diberikan oleh  $1.69 \pm 0.05$  rad dan  $2.09 \pm 0.06$  rad. Kajian ini menyimpulkan bahawa kelayakan sistem fotoakustik untuk memantau perubahan dalam prestasi oksigen tisu sebagai cara alternatif untuk penilaian mudah alih dan pengukuran kepekatan oksigen dalam lingkungan peredaran mikro.

**Kata kunci:** Fotoakustik, sudut fasa, oksigen tisu, peredaran darah, mudah alih

© 2022 Penerbit UTM Press. All rights reserved

## 1.0 INTRODUCTION

Human circulatory system is a network of organs and blood vessels for delivery of nutrients and oxygen, and removal of waste products from the body. This vascular system is controlled by homeostatic mechanisms, which are responsible for maintaining a balanced physiological condition. This is accomplished by the circulating blood, whose main function is to transport oxygen, proteins, nutrients and enzymes to the cells, and to remove carbon dioxide and other waste products from tissues. Hemoglobin is a protein found in red blood cells that is responsible for transport of oxygen in the blood system. A low level of hemoglobin in the blood is a condition known as anemia.

The movement of blood in the human body is affected by flow parameters such as pressure gradient, vessel radius and blood viscosity [1]. The vascular resistance in blood flow increases with the reduced blood vessels' diameter. The latter may be caused by factors such as infections and excessive lipids accumulation. Tissue ischemia, a critical complication related to vascular occlusion, often leads to hypoxia and tissue necrosis. In light of this, many works have been done in the last decades to investigate one's blood oxygen level using Laser Speckle Contrast (LSC) technique [2, 3], Photoplethysmography (PPG) [4], Doppler Flowmetry [5, 6], Spectroscopy [7, 8] and Magnetic Resonance Imaging (MRI) technique [9]. Although these aforementioned systems are noninvasive, each has its own drawbacks. MRI technique offers high diagnostic ability and allows a deeper penetration in tissue, allowing visualization and identification of cancerous tissue (via detection of hypoxia in local micro-environment) located in body cavity. This is at the price of expensive equipment, tedious protocols and long acquisition times [10] while the measurement of LSC is limited to shallow penetration depth of several hundred micrometers below the skin surface [11]. Measurement using PPG device (e.g. pulse oximeter) required the use of a look-up table or a calibration model [12]. The accuracy of pulse oximeter readings is also reported to be compromised in patients with dyshemoglobinemia

(i.e., elevated carboxyhemoglobin and methemoglobin levels) and impaired oxygen saturation. The latter is often linked to poor microcirculation. Meanwhile the application of doppler flowmetry is limited to flow measurement [13]. Spectroscopy is the most commonly used technique for estimation of tissue oxygen saturation level. The measurement is, however, adversely affected by skin pigmentation [14]. Thus, compromising the accuracy of its estimates.

Photoacoustic (PA) imaging has recently emerged as an attractive noninvasive method for light absorption studies [15-17]. This technique combines both optical and acoustic approaches. The measurement procedure of this technique begins with delivery of light energy to the target tissues. Absorption of light in the medium causes thermal expansion in tissues, which is responsible for acoustic wave generation. The waves can be detected using an ultrasonic transducer, and their waveforms can be displayed on an oscilloscope for further signals interpretation and analysis. While pure optical technique adopted in, e.g., spectroscopy and PPG, suffers from strong light scattering in tissues limiting its imaging depth, the effects of scattering on acoustic signal detected by the PA system is two to three orders of magnitude lower than that in prior approach. Thus higher resolution and contrast can be achieved using this hybrid optical/ultrasonic approach [18]. In addition PA modality is free from speckle artifacts, hence it is capable of providing uniform visualization of large volume density of light absorbing units contained within structures with smooth boundaries such as blood vessels filled with hemoglobin [19, 20]. These attributes lead to the use of PA imaging to a wide variety of applications in clinical study [21, 22], preclinical research and basic biology for studying cancer [23-26] and microcirculation [27, 28]. The range of its measurement parameters is mainly depending on the choice of the wavelength and the type of transducer used [21, 26, 29]. The decision on which wavelength to use is made based on wavelength dependent medium's optical properties. Meanwhile the image quality and imaging depth vary with the transducer used (i.e. linear and curved transducer).

The center frequency of the transducer is typically ranged from 1 to 434 MHz for measurement of tissue samples.

Among the state-of-the-art PA systems are the use of a transducer with integrated front end amplifier to simplify the complexity of its prior arts by eliminating optical receiver in the system [30]. The amplifier is to improve the detection sensitivity and to reduce noise. This would, however, increase the cost of the system. In Cao *et al.* [31], a multi-modal system integrating ultrasound, PA and photoacoustic lifetime imaging (PALI) was used to map the distribution of oxygen partial pressure in tissue. Even though the system allows easy and rapid identification of hypoxic regions in tissue samples, it involves high hardware and operation complexity. Besides, its limitations in terms of poor spatial resolution and low penetration depth have not been well addressed. To this end, a multifocal point (MEP) transducer was proposed to provide larger depth of field imaging of tissues in [32]. In another work by Schober and Schwarte [33], a commercial galvanometer scanner with a custom-made scanning mirror was used to improve the spatial resolution of the PA system. Nonetheless, limitations such as bulkiness, non-portability and low compactness remained as the under-explored problems of the conventional PA system that usually comprises of a preamplifier, transducer and oscilloscope for signals detection [34, 35]. Thus, a substantial amount of room is required to house the system. Other applications of PA in the study of tissue characterization and oxygenation include recent works by Fei *et al.* [36] who introduced PA resonance spectroscopy for biological tissues characterization. The workers used the magnitude of PA signal in interpreting the viscosity of the phantoms used. But a high-sensitivity lock-in detection was needed to suppress the background noise and improve the signal-to-noise ratio (SNR). In [37] PA signal was used for characterization of cancer treatment response. This is through the changes in the intensity of two light wavelengths (i.e., 750 nm and 850 nm), which are correlated with changes in tumor oxygenation. It was reported that the sensitivity of acoustic resolution is restricted by the bandwidth of the transducer. The PA signal amplitude was also used for the blood flow measurement in [38, 39]. Phase change value calculated using magnitude information of the measured signal is used to determine the flow rate [36], and for tissues characterization. The quality of the PA images produced following measurement on human forearm was shown in [38] to be superior over ultrasound images during cuff occlusion condition.

Thus far no work has been performed to investigate the relationship between phase angle and tissue oxygen status using PA technique. The phase angle information can be obtained from PA measurement that maps medium absorption characteristics. This paper is inspired to address this gap by manipulating PA signals for measurement of phase shift, and relating the measurement with tissue

oxygen levels. We hypothesize PA phase angle can be a convenient tool for estimation of tissue oxygen content. The objectives of this study are of two folds: (1) to explore the feasibility of using PA phase shift information for detection of microcirculatory function change, and (2) to investigate variability in tissue oxygen induced phase angle among the recruits.

## 2.0 METHODOLOGY

### 2.1 Experimental System and Signal Processing

The PA system designed and assembled in this research consists of a modulated 5 mW HeNe laser emitting light of wavelength 633 nm (R-30993 Newport Corp.) and a light-weight ultrasonic flaw detector of dimensions 23 cm × 16 cm × 7 cm, weighing 1.5 kg in the detection arm as shown in Figure 1 (top). The schematic diagram of this experimental setup is shown at the bottom of the figure.

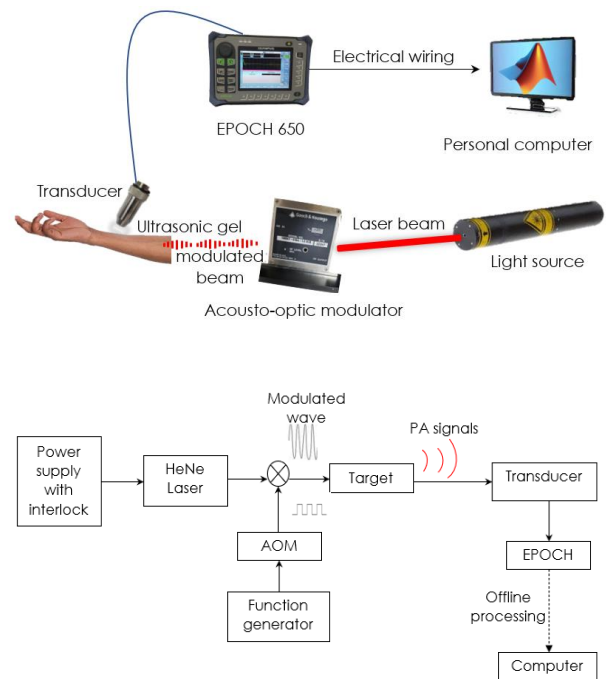


**Figure 1** The experimental equipment (top) and schematic diagram (bottom) of the assembled photoacoustic system

The choice of this wavelength is due to the strong absorption contrast between the hemoglobin components in blood as indicated by the dark vertical bar shown in Figure 2. Since light absorptivity of oxygen deprived hemoglobin (i.e. deoxyhemoglobin, dHb) is higher than that of oxygen rich hemoglobin (i.e. oxyhemoglobin, HbO<sub>2</sub>), greater acoustic pressure is expected to observe in the case of increased dHb concentration as compared to that of HbO<sub>2</sub>.

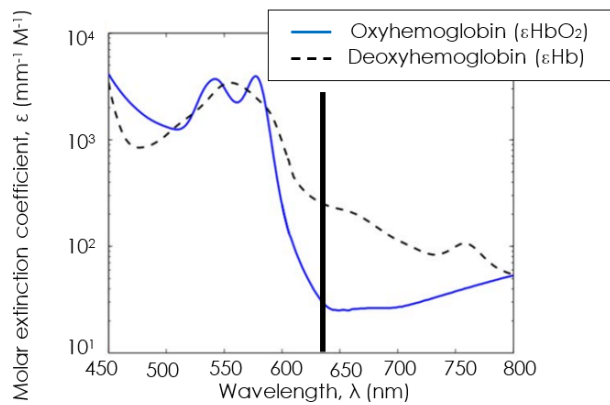


**Figure 2** Wavelength dependent molar extinction coefficient,  $\epsilon$ , of oxyhemoglobin ( $\text{HbO}_2$ ) and deoxyhemoglobin (dHb) from the report of Zijlstra *et al.* [11]. The employed light wavelength value of 633 nm is indicated by the darken bar

The modulated light is produced by passing continuous laser beams through an 80 MHz acousto-optic modulator (AOM) (Gooch & Housego 2910 series). The latter is controlled by a radiofrequency (RF) driver at a carrier frequency of 15 MHz shown in Figure 1 (bottom). The pulsating light propagated in the skin would be absorbed by the medium's absorbers shown in Figure 2, producing thermal expansion in the cavity. This generated changes in pressure propagating through the medium to its surrounding. This signal is collected by a 6 mm diameter flat acoustic linear transducer (V232-SU/2.25 MHz, Olympus NDR). This device detects acoustic waves from the skin depth of approximately 2 cm and displays ultrasonic echo amplitude as a function of time on EPOCH 650 flaw detector (Olympus Corp, Japan). Ultrasonic gel was applied generously on the investigated site in Figure 1 (top) to establish an effective acoustic coupling between the skin and transducer head prior to the measurement.

This study uses phase angle information to deduce changes in tissue hemodynamic status with external interventions. This information can be calculated from the real (cosine) and imaginary parts (sine functions) of acoustic signals [36]. In the present study, Fast Fourier Transform (FFT) algorithm is used to deconvolute complex acoustic signals into its sine and cosine components. This function is available in MATLAB®: *fft()* shown in Equation 1.

$$(\Psi_{re}, \Psi_{im}) = \text{fft}(\psi(t)) \quad (1)$$

where  $\psi(t)$  represents echo amplitude in time domain, while  $\Psi_{re}$  and  $\Psi_{im}$  denote real and imaginary parts of the acoustic spectrum. Using these real and imaginary components, the required phasor quantity (i.e. phase angle of the signal) is given by:

$$\theta = \tan^{-1}\left(\frac{\Psi_{im}}{\Psi_{re}}\right) \quad (2)$$

## 2.2 Subjects and Protocol

Six healthy volunteers (three male and three females aged between 26 - 30 years) were recruited for this preliminary research. This study is approved by Research Ethics Committee of Universiti Tun Hussein Onn Malaysia (RMC.100-9/39,5). These volunteers were referred in the following as volunteer index A - F. They declared no known serious illness and were briefed on the experiment procedures, purpose, and possible risks prior to the experiment. They were told to sign informed consent form upon enrollment. The experiment was conducted under three conditions, namely at rest condition, diastolic and systolic occlusions to induce microcirculatory change in the left anterior forearm of the volunteers. These considered pressures are to promote different degree of blood flow obstruction, and hence changes in microcirculatory function, in the investigated arm. These changes in the recruits' tissue oxygen levels were verified using market available finger pulse oximeter (model no. X1805). The average blood oxygen saturation measured from the index finger of the investigated arm was recorded as 98 %, 95.6 % and 93.3 %, respectively, for at rest, diastolic and systolic occlusions.

This study began with at rest condition, where each subject was instructed to place the investigated site under illumination of modulated beams. Two measurements were conducted with 10 seconds intervening. In each measurement three readings were consecutively collected. In the case of diastolic occlusion, a manual blood pressure cuff was used to induce ischemia at the upper left arm of each subject by exerting a pressure of 80 mmHg. This study allocated 10 seconds waiting time for maintaining microcirculatory disturbance after occlusion before data were collected every 10 seconds for 50 seconds. Without the inflated cuff released, systolic pressure of 120 mmHg was applied for 60 seconds. Similar to the earlier experiment, 10 seconds waiting time was allowed before the spectrum was recorded. Under both occlusion condition, experiment would be immediately terminated upon complaints of pain in the occluded arm by the subjects shown in Figure 3. The transducer head was placed in contact with the skin throughout the measurement as shown in Figure 1 and the signals were recorded at the time specified above using the digital ultrasonic flaw detector. These signals stored in a microSD memory card were used for further offline manipulation and analysis. The flow chart of the experimental procedure is shown in Figure 3.

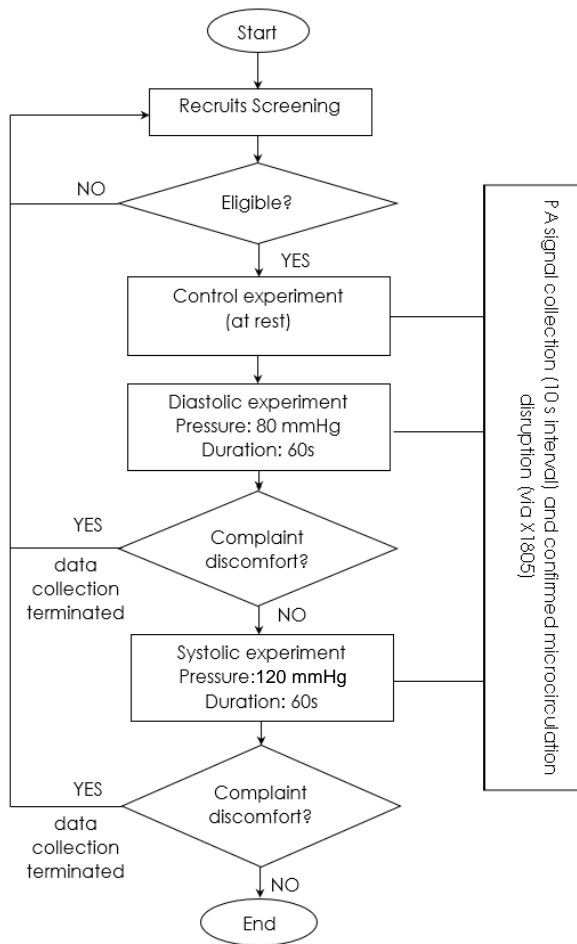


**Figure 3** Flow chart of the experimental procedure

### 3.0 RESULTS AND DISCUSSION

An example of echoes measured from one of the volunteers under the considered experimental conditions are shown in Figure 4. The diffraction and natural frequency response of the transducer (between time 50 and 130  $\mu\text{s}$ ) were removed, and the rest of the spectrum (indicated by red box in Figure 4) is used for calculation of phase angle changes. Since each measurement was run for three times, the mean and STDEV of phase angles were calculated for different acquisition time as described in protocol and plotted in Figure 4. The difference between the phase angles calculated for at rest, diastolic and systolic occlusions in Figure 5 is statistically tested using a one-way ANOVA test in SPSS Statistics version 26 with confidence level of 95 %. The results showed significance value,  $p$ , of 0.000 for the relationship between means of phase angle and the experimental conditions. This implies the null hypothesis that the means of phase angle are equal for all the experimental conditions cannot be supported. Meanwhile  $p = 0.000$  is calculated for investigation of variability in measurement between

different subjects, suggesting statistically significance of difference between signals from different individuals.

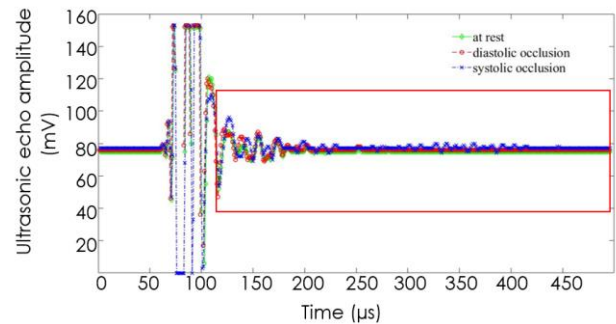


**Figure 4** The measured ultrasonic amplitude spectrum for one of the subjects under different experimental condition. The signals within the region marked by the red box are used for evaluation of phase angle change

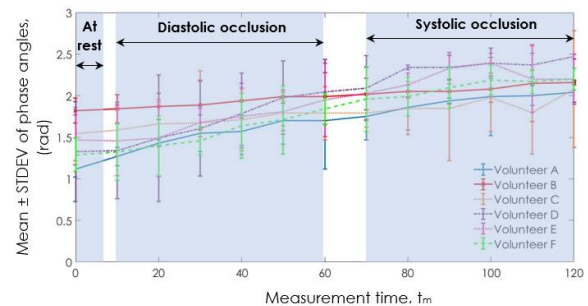


**Figure 5** The mean and standard deviation (STDEV) of phase angles calculated from photoacoustic spectrum collected from six human subjects (volunteer A-F) at different measurement time ( $t_m$ ) and under different microcirculatory disturbances

Figure 5 reveals a consistently low phase angles ranged between 1.12 – 1.82 rads measured for all subjects under at rest condition ( $t_m = 0$  and 10 seconds). This is followed by an overall gradual increasing trend in the calculated value with intensity in the microcirculation disruption, wherein the average mean and STDEV of phase angle are given by  $1.69 \pm 0.05$  rads and  $2.09 \pm 0.06$  rads, respectively, for diastolic and systolic occlusions. A statistically significant difference ( $p < 0.05$ ) is observed between groups with different microcirculatory performance. This is supported by the results of [33, 40], where a linear correlation between blood perfusion and tissue oxygenation in the body was reported. The ischemic pressures applied on the upper arm resisted the oxygenated blood from flowing into the lower limb, impairing delivery of oxygen and causing an increased accumulation of carbon dioxide in the tissue. This causes a rise in the level of dHb in Figure 2. The generation of acoustic energy in a medium is proportional to the light absorptivity [41], thus our findings in Figure 5 support the research hypothesis

that phase angle magnitude would increase with the induced ischemic condition.

This study also reports statistically significant results between the mean values of signals from the six recruits ( $p = 0.000$ ). Nonetheless, visual examination of the results of Figure 5 showed considerably small change in phase angle in volunteer B. A further investigation into her medical record and history revealed that the subject experience mild anemia. Her laboratory report showed hemoglobin count of 10.5 g/dl, which is lower than the normal range [42]. The normal range of hemoglobin for female and male is given by 12.0 to 15.5 g/dl and 13.5 to 17.5 g/dl, [43] respectively. A low hemoglobin concentration causes low oxygen carrying capacity [44]. In the case of patients with chronic anemia, this results in an increased capillary permeability and subsequently higher tolerance of capillary wall to anoxia [45]. So, this could possibly be one of the key reasons for the insignificant change in the acoustic echoes measured for the aforementioned subject under occlusion conditions. Even though the recent medical record of volunteer A (dated 9<sup>th</sup> September 2020) also shows relatively low hemoglobin level of 10.2 g/dl, the subject started taking folic acid supplements one time daily for a month prior to the experiment. This multivitamin supplement encourages iron absorption and hence promotes hemoglobin production [46]. This is evident in the more pronounced increasing trend in the phase change in volunteer A as compared to its counterpart.

The volunteer C, D, E and F have normal hemoglobin count given by 13.4 g/dl, 15.9 g/dl, 15.6 g/dl and 14.9 g/dl, respectively. When comparing the findings in Figure 5, our observations suggest that the results of volunteer D can be regarded as the most ideal followed by volunteer F. This is because of the most significant change in the magnitude of its acoustic echoes produced with the application of cuff pressures, and following the increase in dHb level. Some inconsistencies in the phase changes shown in Figure 5 (e.g., between  $t_m = 0$  and 10 s in Volunteer A and  $t_m = 110$  s and 120 s in Volunteer E) may be due to either the motion artifacts or noise in the system. It is also interesting to note that results of volunteer C showed a similar trend as that of volunteer B. This may be contributed by physiological conditions of this subject, wherein the subject was having menstruation during the time of measurements. Previous report in [43] showed that the hemoglobin concentration decreased during menstruation as compared to ovulation. Thus, producing similar effects as that in mild anemic case.

Even though this study is not able to provide direct estimation of tissue oxygen saturation values such as that demonstrated in previous works [8] that used a considerably wide wavelength range of 650 nm – 970 nm, the phase angles found in this study may provide a crude but useful indication of tissue health status. This parameter may also be used to quantify perfusion and oxygen delivery-consumption balance in microcirculatory environment.

This work concluded that the PA phase information may be used for monitoring of hemodynamic changes and microcirculatory performance for wide applications such as wound care and postoperative management. The future of this work includes the use of an isosbestic wavelength (e.g. 532 nm in Figure 2) for signals normalization. This may help to minimize the PA effects produced by other tissue chromophores (e.g. melanosomes in skin), and enhance phase contrast induced by hemodynamic activities. Meanwhile a mechanical arm and padded support may be adopted in future design to hold the transducer steady on the subject's skin, and to reduce motion artifacts during data acquisition. This is in addition to the use of adaptive algorithms to enhance signal quality.

## 4.0 CONCLUSION

As a concluding remark, this work confirms the feasibility of using an ultrasonic flaw detector for measurement of PA phase angle to monitor skin tissue oxygen. This study observed a gradual increase in the calculated phase angle from  $1.43 \pm 0.06$  rads during at rest to  $2.09 \pm 0.06$  rads in systolic occlusions measured for all subjects. We attribute the inconsistency in the increasing rate of phase angle ( $p = 0.0017$ ) to differences in health of individuals participated in this research and motion artifacts during the experiment. The preliminary findings from this study contribute to the knowledge in terms of advancing understanding of alternative portable methods for in-vivo monitoring of microcirculation. In future, a predictive model relating the PA phase angle and tissue oxygen levels, formulated from a larger subject sample, would be proposed to allow online prediction of oxygen status. The measurement could also be enhanced by upgrading experimental techniques, and signal processing strategies.

## Acknowledgement

This research was supported by the Ministry of Higher Education (MOHE) Malaysia through Fundamental Research Grant Scheme (FRGS/1/2020/TK0/UTHM/02/28).

## References

- [1] K. A. Y. J. Gordon Betts, James A. Wise, Eddie Johnson, Brandon Poe, Dean H. Kruse, Oksana Korol, Jody E. Johnson, Mark Womble, Peter DeSaix. 2013. *Anatomy and Physiology Module 4: The Cardiovascular System: Blood Vessels and Circulation*. OSCRice University. OpenStax. DOI: ISSN 9781947172043 1947172042
- [2] R. Reif, J. Qin, L. Shi, S. Dziennis, Z. Zhi, A. L. Nuttall, et al. 2012. Monitoring Hypoxia Induced Changes in Cochlear Blood Flow and Hemoglobin Concentration using a Combined Dual-wavelength Laser Speckle Contrast

- Imaging and Doppler Optical Microangiography System. *PLoS one*. 7: e25041.  
DOI: <https://doi.org/10.1371/journal.pone.0052041>.
- [3] C. Y. Lee, B.-H. Huang, W. J. Chen, J. Y. Yi, and M. T. Tsai. 2020. Microscope-type Laser Speckle Contrast Imaging for In Vivo Assessment of Microcirculation. *OSA Continuum*. 3(5): 1129-1137.  
DOI: <https://doi.org/10.1364/OSAC.389560>.
- [4] D. McDuff, I. Nishidate, K. Nakano, H. Haneishi, Y. Aoki, C. Tanabe, et al. 2020. Non-contact Imaging of Peripheral Hemodynamics during Cognitive and Psychological Stressors. *Scientific Reports*. 10: 1-13. DOI: <https://doi.org/10.1038/s41598-020-67647-6>.
- [5] A. A. Mendelson, A. Rajaram, D. Bainbridge, K. S. Lawrence, T. Bentall, M. Sharpe, et al. 2020. Dynamic Tracking of Microvascular Hemoglobin Content for Continuous Perfusion Monitoring in the Intensive Care Unit: Pilot Feasibility Study. *Journal of Clinical Monitoring and Computing*. 1-13.  
DOI: <https://doi.org/10.1007/s10877-020-00611-x>.
- [6] D. Bender, S. Tweer, F. Werdin, J. Rothenberger, A. Daigeler, and M. Held. 2020. The Acute Impact of Local Cooling Versus Local Heating on Human Skin Microcirculation using Laser Doppler Flowmetry and Tissue Spectrophotometry. *Burns*. 46: 104-109.  
DOI: <https://doi.org/10.1016/j.burns.2019.03.009>.
- [7] K. Goeral, B. Urlesberger, V. Giordano, G. Kaspran, M. Wagner, L. Schmidt, et al. 2017. Prediction of Outcome in Neonates with Hypoxic-ischemic Encephalopathy II: Role of Amplitude-integrated Electroencephalography and Cerebral Oxygen Saturation Measured by Near-infrared Spectroscopy. *Neonatology*. 112(3): 193-202.  
DOI: <https://doi.org/10.1159/000468976>.
- [8] K. Steenhaut, K. Lapage, T. Bove, S. De Hert, and A. Moerman. 2017. Evaluation of Different Near-infrared Spectroscopy Technologies for Assessment of Tissue Oxygen Saturation during a Vascular Occlusion Test. *Journal of Clinical Monitoring and Computing*. 31: 1151-1158. DOI: <https://doi.org/10.1159/000468976>.
- [9] P. Eckerbom, P. Hansell, E. F. Cox, C. E. Buchanan, J. Weis, F. Palm, et al. 2020. Circadian Variation in Renal Blood Flow and Kidney Function in Healthy Volunteers Monitored using Non-invasive Magnetic Resonance Imaging. *American Journal of Physiology-Renal Physiology*. 319(6): F966-F978.  
DOI: <https://doi.org/10.1152/ajprenal.00311.2020>.
- [10] X. Dang, N. M. Bardhan, J. Qi, L. Gu, N. A. Eze, C.-W. Lin, et al. 2019. Deep-tissue Optical Imaging of Near Cellular-sized Features. *Scientific Reports*. 9(1): 1-12.  
DOI: <https://doi.org/10.1038/s41598-019-39502-w>.
- [11] N. Li, K. Murari, A. Rege, P. Miao, and N. Thakor. 2009. Multifunction-laser Speckle Blood Flow and Deoxy-hemoglobin Saturation-Imaging of Cerebrovascular Response. *4th International IEEE/EMBS Conference on Neural Engineering*. 241-244.  
DOI: <https://doi.org/10.1109/NER.2009.5109278>.
- [12] M. Nitzan, S. Noach, E. Tobal, Y. Adar, Y. Miller, E. Shalom, et al. 2014. Calibration-free Pulse Oximetry based on Two Wavelengths in the Infrared—A Preliminary Study. *Sensors*. 14(4): 7420-7434.  
DOI: <https://doi.org/10.3390/s140407420>.
- [13] N. Pouratian. 2002. Optical Imaging based on Intrinsic Signals. *Brain Mapping*. 97-140.  
DOI: <https://doi.org/10.1016/B978-012693019-1/50007-1>.
- [14] L. Couch, M. Roskosky, B. A. Freedman, and M. S. Shuler. 2015. Effect of skin pigmentation on near infrared spectroscopy. *American Journal of Analytical Chemistry*. 6(12): 911.  
DOI: <https://doi.org/10.4236/ajac.2015.612086>.
- [15] P. Cheng, W. Chen, S. Li, S. He, Q. Miao, and K. Pu. 2020. Fluoro-Photoacoustic Polymeric Renal Reporter for Real-time Dual Imaging of Acute Kidney Injury. *Advanced Materials*. 32: 1908530.  
DOI: <https://doi.org/10.1002/adma.201908530>.
- [16] Y. Zhu, L. A. Johnson, J. M. Rubin, H. Appelman, L. Ni, J. Yuan, et al. 2019. Strain-photoacoustic Imaging as a Potential Tool for Characterizing Intestinal Fibrosis. *Gastroenterology*. 157: 1196-1198.  
DOI: <https://doi.org/10.1053/j.gastro.2019.07.061>.
- [17] T. Han, M. Yang, F. Yang, L. Zhao, Y. Jiang, and C. Li. 2020. A Three-dimensional Modeling Method for Quantitative Photoacoustic Breast Imaging with Handheld Probe. *Photoacoustics*. 100222.  
DOI: <https://doi.org/10.1016/j.pacs.2020.100222>.
- [18] M. Xu and L. V. Wang. 2006. Photoacoustic Imaging in Biomedicine. *Review of Scientific Instruments*. 77: 041101.  
DOI: <https://doi.org/10.1063/1.2195024>.
- [19] Z. Guo, L. Li, and L. V. Wang. 2009. On the Speckle-free Nature of Photoacoustic Tomography. *Medical Physics*. 36: 4084-4088. DOI: <https://doi.org/10.1118/1.3187231>.
- [20] J. Gateau, T. Chaigne, O. Katz, S. Gigan, and E. Bossy. 2013. Improving Visibility in Photoacoustic Imaging using Dynamic Speckle Illumination. *Optics Letters*. 38: 5188-5191.  
DOI: <https://doi.org/10.1364/OL.38.005188>.
- [21] J. L. Su, A. B. Karpiouk, B. Wang, and S. Y. Emelianov. 2010. Photoacoustic Imaging of Clinical Metal Needles in Tissue. *Journal of Biomedical Optics*. 15: 021309.  
DOI: <https://doi.org/10.1117/1.3368686>.
- [22] W. Choi, E.-Y. Park, S. Jeon, and C. Kim. 2018. Clinical Photoacoustic Imaging Platforms. *Biomedical Engineering Letters*. 8: 139-155.  
DOI: <https://doi.org/10.1007/s13534-018-0062-7>.
- [23] T. Temma, S. Onoe, K. Kanazaki, M. Ono, and H. Saji. 2014. Preclinical Evaluation of a Novel Cyanine Dye for Tumor Imaging with in Vivo Photoacoustic Imaging. *Journal of Biomedical Optics*. 19: 090501.  
DOI: <https://doi.org/10.1117/1.JBO.19.9.090501>.
- [24] S. Mallidi, G. P. Luke, and S. Emelianov. 2011. Photoacoustic Imaging in Cancer Detection, Diagnosis, and Treatment Guidance. *Trends in Biotechnology*. 29: 213-221.  
DOI: <https://doi.org/10.1016/j.tibtech.2011.01.006>.
- [25] R. A. Kruger, R. B. Lam, D. R. Reinecke, S. P. Del Rio, and R. P. Doyle. 2010. Photoacoustic Angiography of the Breast. *Medical Physics*. 37: 6096-6100.  
DOI: <https://doi.org/10.1118/1.3497677>.
- [26] N. Nyayapathi, R. Lim, H. Zhang, W. Zheng, Y. Wang, M. Tiao, et al. 2019. Dual Scan Mammoscope (DSM)—A New Portable Photoacoustic Breast Imaging System with Scanning in Craniocaudal Plane. *IEEE Transactions on Biomedical Engineering*. 67: 1321-1327.  
DOI: <https://doi.org/10.1109/TBME.2019.2936088>.
- [27] Y. Zhu, X. Lu, X. Dong, J. Yuan, M. L. Fabiilli, and X. Wang. 2019. LED-based Photoacoustic Imaging for Monitoring Angiogenesis in Fibrin Scaffolds. *Tissue Engineering Part C: Methods*. 25: 523-531.  
DOI: <https://doi.org/10.1089/ten.tec.2019.0151>.
- [28] J. Yao, J. Xia, K. I. Maslov, M. Nasirivanaki, V. Tsytarev, A. V. Demchenko. 2013. Noninvasive Photoacoustic Computed Tomography of Mouse Brain Metabolism in Vivo. *Neuroimage*. 64: 257-266.  
DOI: <https://doi.org/10.1016/j.neuroimage.2012.08.054>.
- [29] D. Piras, W. Xia, W. Steenbergen, T. G. van Leeuwen, and S. Manohar. 2010. Photoacoustic Imaging of the Breast using the Twente Photoacoustic Mammoscope: Present Status and Future Perspectives. *IEEE Journal of Selected Topics in Quantum Electronics*. 16: 730-739.  
DOI: <https://doi.org/10.1109/JSTQE.2009.2034870>.
- [30] C. Yang, X. Jian, X. Zhu, J. Lv, Y. Jiao, Z. Han, et al. 2020. Sensitivity Enhanced Photoacoustic Imaging Using a High-Frequency PZT Transducer with an Integrated Front-End Amplifier. *Sensors*. 20: 766.  
DOI: <https://doi.org/10.3390/s20030766>.
- [31] F. Cao, Z. Qiu, H. Li, and P. Lai. 2017. Photoacoustic Imaging in Oxygen Detection. *Applied Sciences*. 7: 1262.  
DOI: <https://doi.org/10.3390/app7121262>.
- [32] T. P. Nguyen, V. T. Nguyen, S. Mondal, V. H. Pham, D. D. Vu, B.-G. Kim, et al. 2020. Improved Depth-of-Field

- Photoacoustic Microscopy with a Multifocal Point Transducer for Biomedical Imaging. *Sensors*. 20. DOI: <https://doi.org/10.3390/s20072020>.
- [33] P. Schober and L. A. Schwarte. 2012. From System to Organ to Cell: Oxygenation and Perfusion Measurement in Anesthesia and Critical Care. *Journal of Clinical Monitoring and Computing*. 26: 255-265. DOI: <https://doi.org/10.1007/s10877-012-9350-4>.
- [34] F. Gao, X. Feng, and Y. Zheng. 2014. Photoacoustic Phasoscopy Super-contrast Imaging Correlating Optical Absorption and Scattering. *Photons Plus Ultrasound: Imaging and Sensing 2014*. 89435L. DOI: <https://doi.org/10.1117/12.2041867>.
- [35] Y. Zhou, J. Yao, and L. V. Wang. 2016. Tutorial on Photoacoustic Tomography. *Journal of Biomedical Optics*. 21: 061007. DOI: <https://doi.org/10.1117/1.JBO.21.6.061007>.
- [36] F. Gao, X. Feng, Y. Zheng, and C.-D. Ohl. 2017. Photoacoustic Resonance Spectroscopy for Biological Tissue Characterization. *Journal of Biomedical Optics*. 19: 067006. DOI: <https://doi.org/10.1117/1.JBO.19.6.067006>.
- [37] E. Hysi, L. A. Wirtzfeld, J. P. May, E. Undzys, S.-D. Li, and M. C. Kolios. 2017. Photoacoustic Signal Characterization of Cancer Treatment Response: Correlation with Changes in Tumor Oxygenation. *Photoacoustics*. 5: 25-35. DOI: <https://doi.org/10.1016/j.pacs.2017.03.003>.
- [38] Jinge, Y., Guang, Z., Wu, C., Zihui, C., Qiquan, S., Man, W., et al. 2020. Photoacoustic Imaging of Hemodynamic Changes in Foreman Skeletal Muscle during Cuff Occlusion. *Biomedical Optics Express*. 11(8): 4560-4570. DOI: <https://doi.org/10.1364/BOE.392221>.
- [39] H. Zhao, Y. Liu, T. Farooq, and H. Fang. 2021. Dual-Wavelength Continuous Wave Photoacoustic Doppler Flow Measurement. *Photonic Sensors*. 1-9. DOI: <https://doi.org/10.1007/s13320-021-0633-6>.
- [40] R. N. Pittman. 2011. The Circulatory System and Oxygen Transport. *Regulation of Tissue Oxygenation*. Morgan & Claypool Life Sciences. 3(3): 1-100. DOI: <https://doi.org/10.4199/C00029ED1V01Y201103ISP017>.
- [41] J. R. Rajian, P. L. Carson, and X. Wang. 2009. Quantitative Photoacoustic Measurement of Tissue Optical Absorption Spectrum Aided by an Optical Contrast Agent. *Optics Express*. 17: 4879-4889. DOI: <https://doi.org/10.1364/OE.17.004879>.
- [42] T. Jewell. 2019. Hemoglobin (HGB) Test Results. U.S. Department of Health and Human Services National Institutes of Health.
- [43] M. D. Scott Litin. 2019. Hemoglobin Test. Mayo Foundation for Medical Education and Research (MFMER).
- [44] C. E. Rhodes and M. Varacallo. 2019. Physiology, Oxygen Transport. *StatPearls*. StatPearls Publishing. DOI: <https://www.ncbi.nlm.nih.gov/books/NBK538336/>
- [45] L. Claesson-Welsh. 2015. Vascular Permeability—The Essentials. *Upsala Journal of Medical Sciences*. 120: 135-143. DOI: <https://doi.org/10.3109/03009734.2015.1064501>.
- [46] M. A. Abu, A. S. Borhan, A. K. A. Karim, M. F. Ahmad, and Z. A. Mahdy. 2020. Comparison between Iberet Folic® and Zincofer® in Treatment of Iron Deficiency Anaemia in Pregnancy. *Hormone Molecular Biology and Clinical Investigation*. 42(1): 49-56. DOI: <https://doi.org/10.1515/hmbci-2020-0034>.